Electronic supplementary information for

Solvent selection as a major determinant of chiral resolution outcomes: The BINOL-DACH case study

Joséphine de Meester, Oleksii Shemchuk, Laurent Collard, Johan Wouters, Koen Robeyns, Tom Leyssens*

*Corresponding author: tom.leyssens@uclouvain.be

Table of Contents

Interactions with solvents

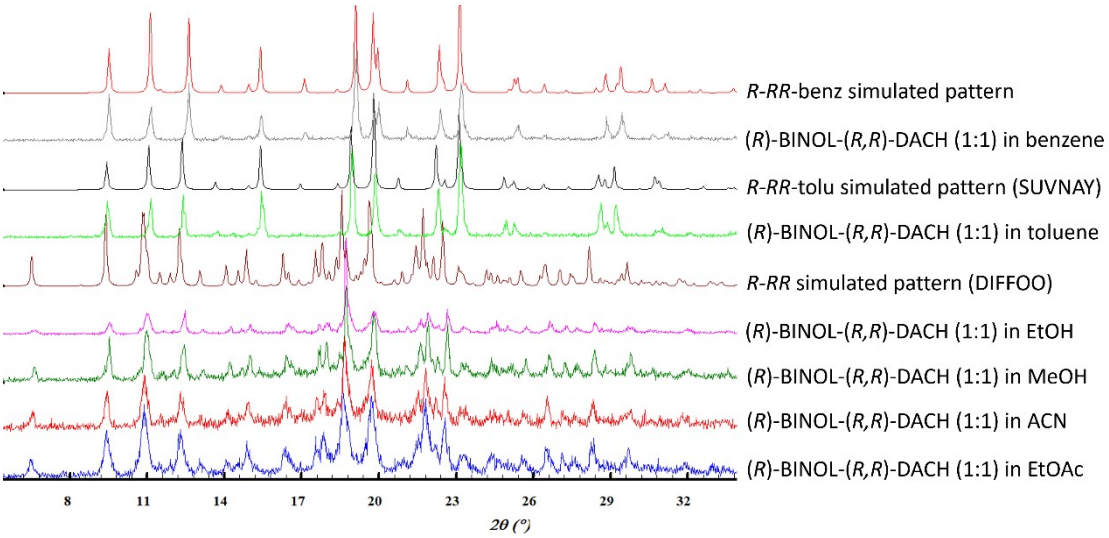

Figure SI-1. Comparison of the X-ray diffraction patterns between slurry outcomes of (*R*)-BINOL and (*R,R*)-DACH in different solvents.

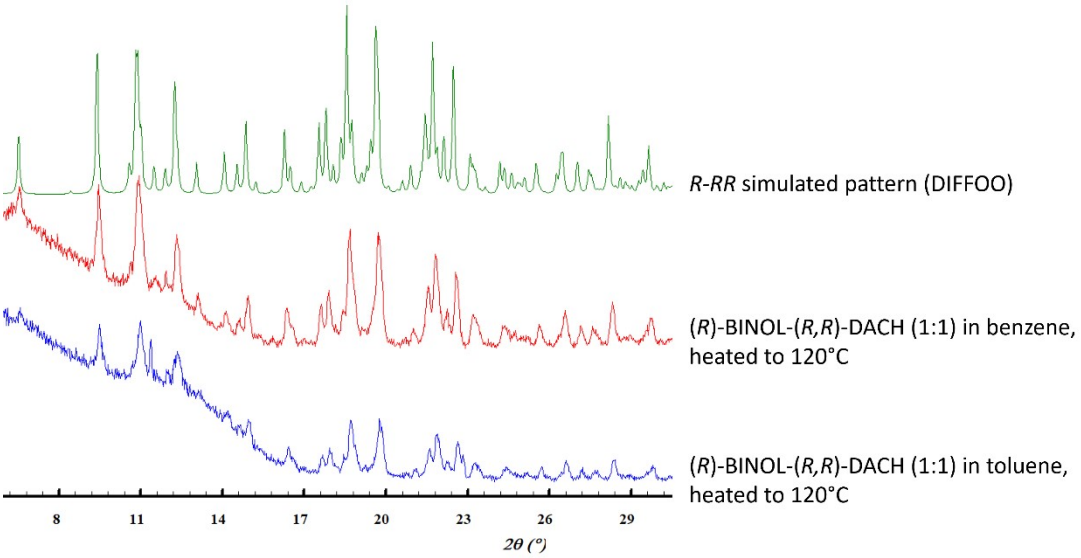

Figure SI-2. Comparison of the X-ray diffraction patterns of *R-RR*-tolu and *R-RR*-benz, each heated to 120°C, with the *R-RR* cocrystal.

a

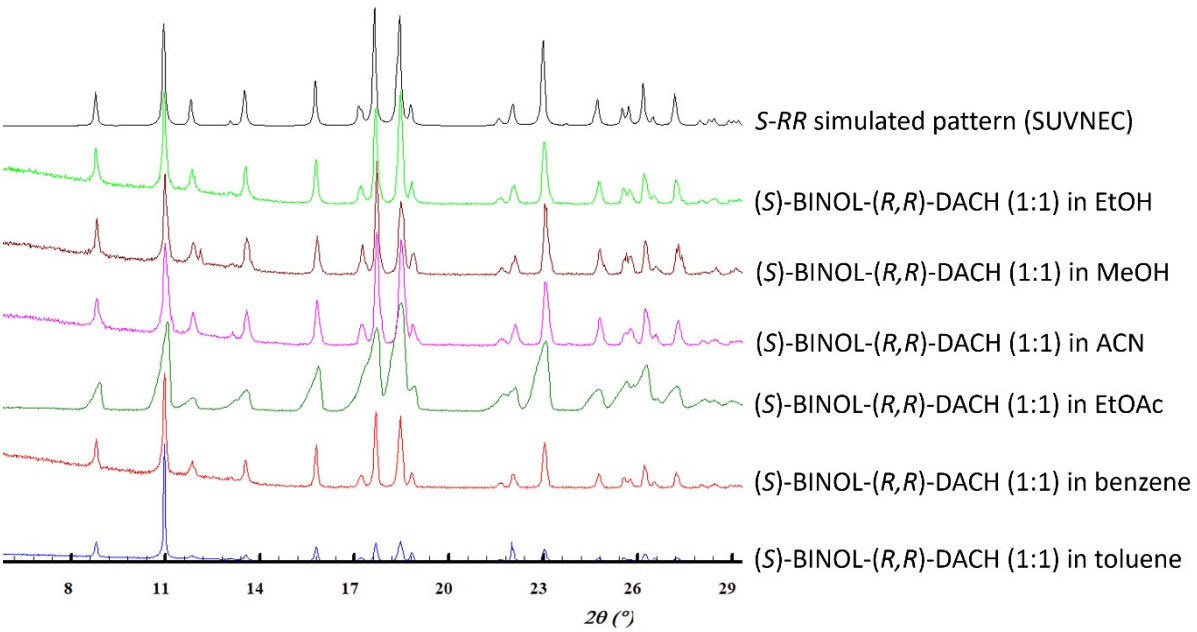

Figure SI-3. Comparison of the X-ray diffraction patterns between the slurry outcome of (*S*)-BINOL and (*R,R*)-DACH in different solvents.

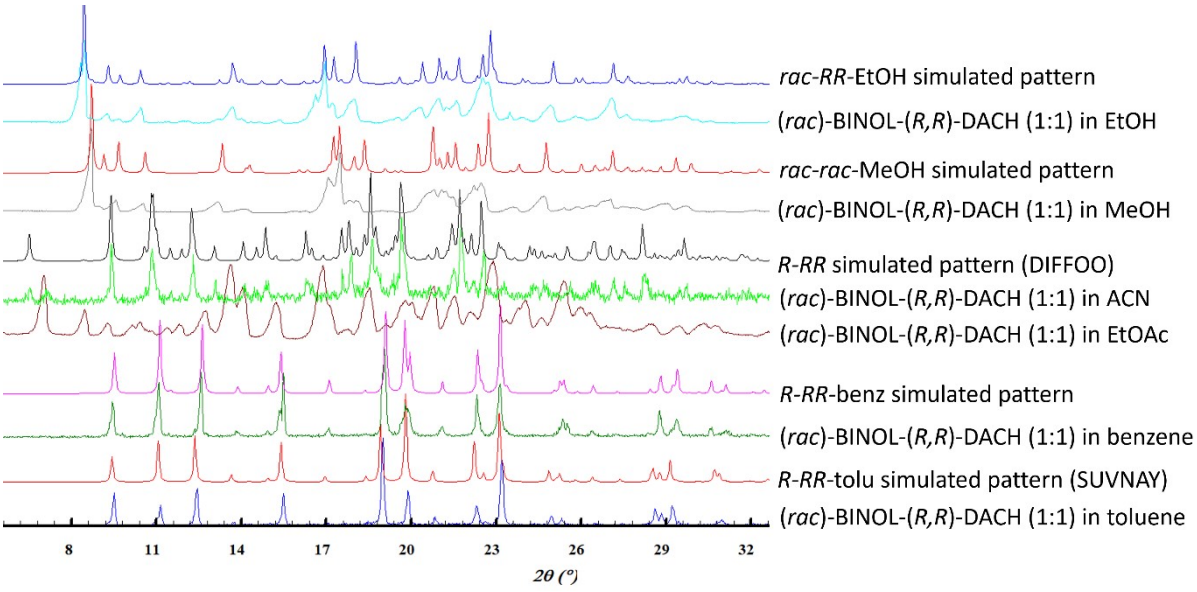

Figure SI-4. Comparison of the X-ray diffraction patterns between slurry outcomes of (*rac*)-BINOL and (*R,R*)-DACH in different solvents.

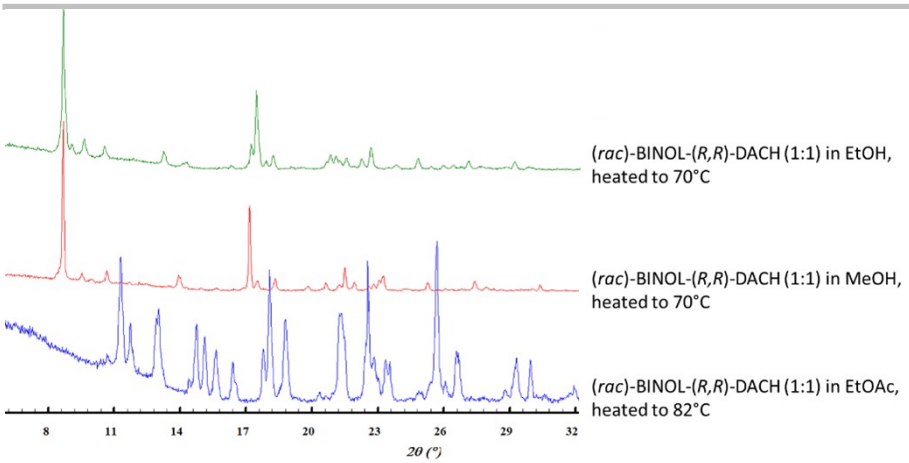

Figure SI-5. Comparison of the X-ray diffraction patterns of the powders recovered by slurrying *(rac)*-BINOL and *(R,R)*-DACH in EtOAc, MeOH and EtOH, heated to respectively 82°C, 70°C, and 70°C.

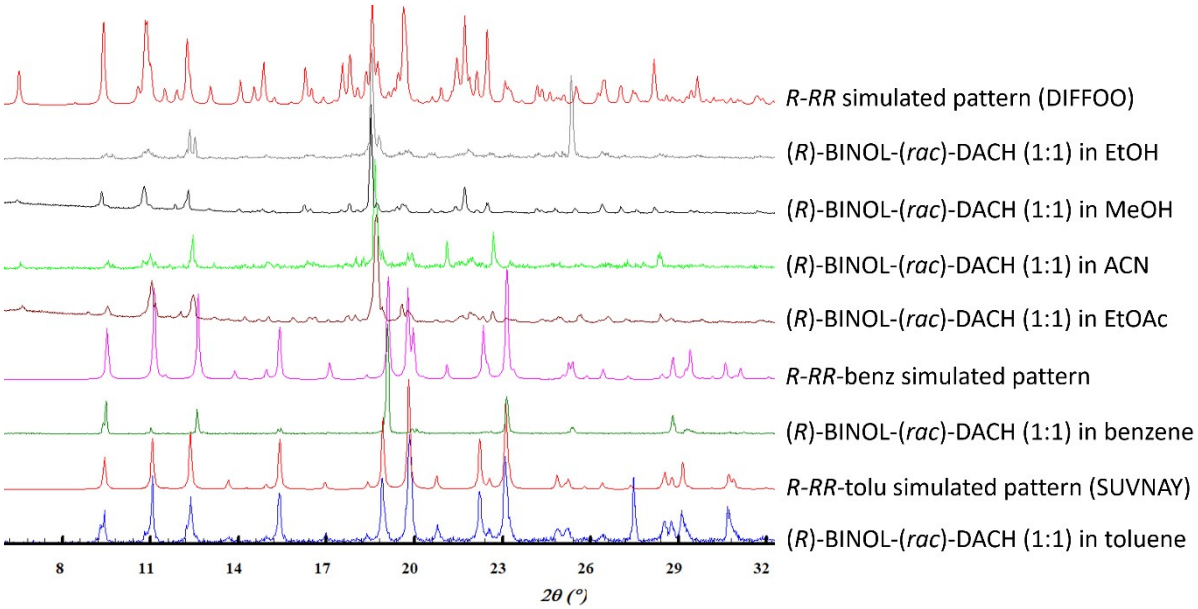

Figure SI-6. Comparison of the X-ray diffraction patterns between slurry outcomes of (*R*)-BINOL and (*rac*)-DACH in different solvents.

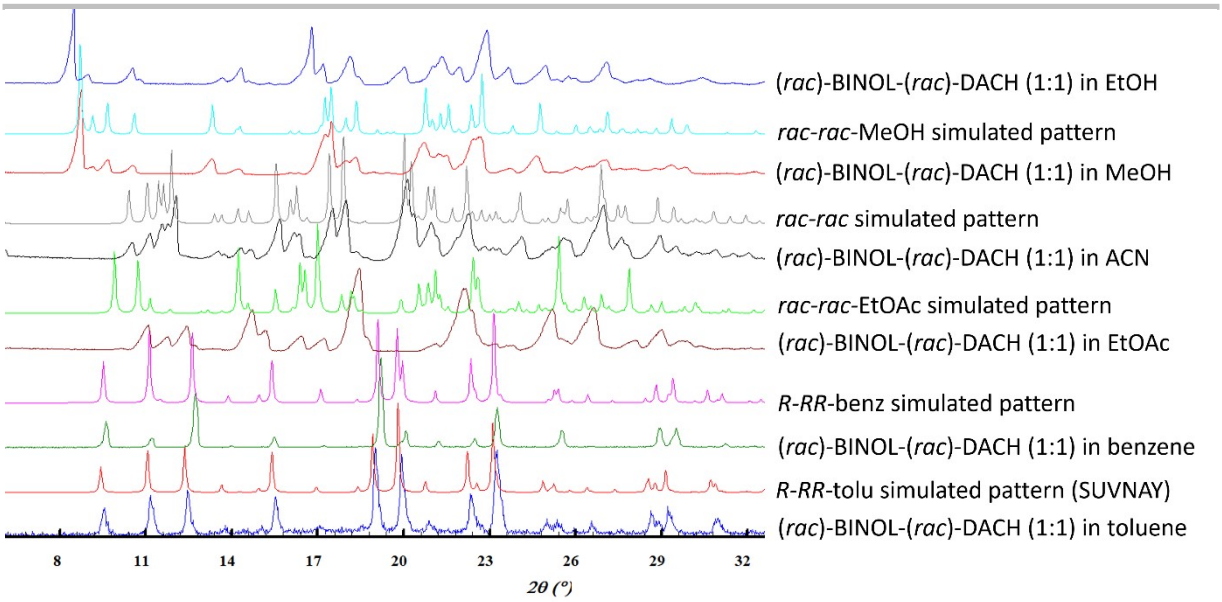

Figure SI-7. Comparison of the X-ray diffraction patterns between slurry outcomes of (*rac*)-BINOL and (*rac*)-DACH in different solvents.

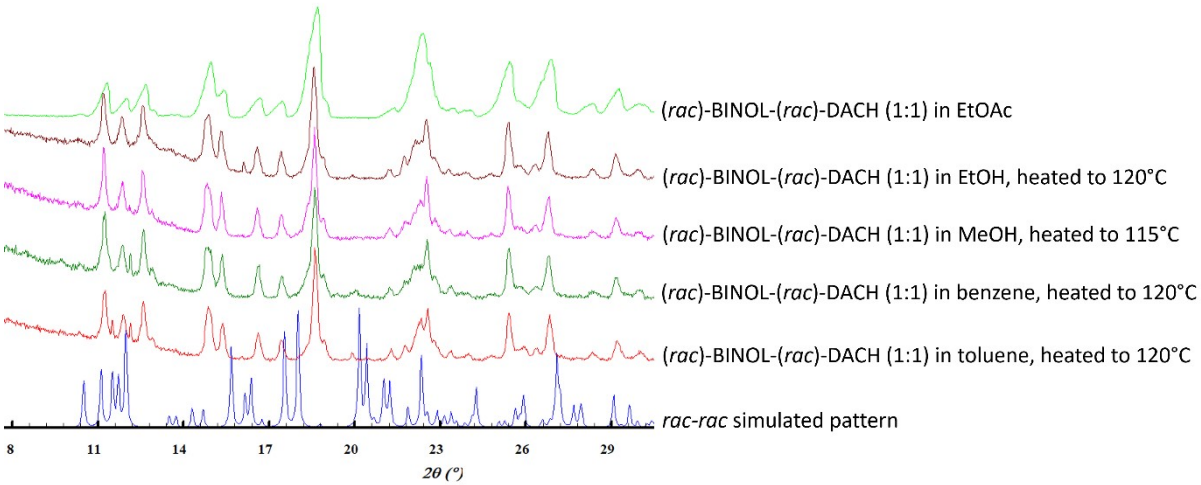

Figure SI-8. Comparison of the X-ray diffraction patterns of the powders recovered by slurrying *(rac)*-BINOL and *(rac)*-DACH in toluene, benzene, MeOH and EtOH, heated to respectively 120°C, 120°C, 115°C, and 120°C, with the outcome of the slurry (*rac)*-BINOL and *(rac)*-DACH in EtOAc and the *rac-rac* simulated pattern, obtained in ACN.

Structural analysis

Table SI-1. Crystallographic data and structure refinement details for *R-RR*, *R-RR*-benz, 4*rac*-4*RR*-3EtOH-H_2O, *rac-rac*-EtOAc, *rac-rac* and *rac-rac*-MeOH phases.

Identification code	**(*R*)-BINOL-(*R,R*)DACH *R-RR***	**(*R*)-BINOL-(*R,R*)-DACH-benzene *R-RR*-benz**	**4(*rac*)-BINOL-4(*R,R*)-DACH-3EtOH-H_2O 4*rac*-4*RR*-3EtOH-H_2O**
Empirical formula	$C_{26}H_{28}N_2O_2$	$C_{32}H_{34}N_2O_2$	$C_{110}H_{132}N_8O_{12}$
Formula weight [g/mol]	400.50	478.61	1758.23
Temperature [K]	150(2)	297(2)	297(2)
Crystal system	orthorhombic	orthorhombic	triclinic
Space group	$P2_12_12_1$	$C222_1$	$P1$
a [Å]	9.85511(18)	12.3993(15)	10.3936(12)
b [Å]	15.3092(3)	14.0194(10)	11.2508(9)
c [Å]	28.2920(6)	15.3719(12)	20.951(2)
α [°]	90	90	87.176(7)
β [°]	90	90	89.274(8)
γ [°]	90	90	76.533(8)
Volume [Å^3]	4268.53(15)	2672.1(4)	2379.6(4)
Z	8	4	1
ρ_{calc} [g/cm^3]	1.246	1.190	1.227
μ [mm^{-1}]	0.079	0.074	0.080
F(000)	1712.0	1024.0	944.0
Crystal size [mm^3]	0.4 × 0.27 × 0.04	0.2 × 0.02 × 0.01	0.12 × 0.1 × 0.1
Radiation	MoKα (λ = 0.71073)	MoKα (λ = 0.71073)	MoKα (λ = 0.71073)
2Θ range for data collection [°]	5.98 to 52.304	6.388 to 46.452	5.122 to 50.504
Index ranges	-12 ≤ h ≤ 12, -18 ≤ k ≤ 18, -34 ≤ l ≤ 35	-13 ≤ h ≤ 13, -15 ≤ k ≤ 15, -16 ≤ l ≤ 16	-12 ≤ h ≤ 12, -13 ≤ k ≤ 13, -25 ≤ l ≤ 25
Reflections collected	37239	7721	41911
Independent reflections	8486 [R_{int} = 0.0484, R_{sigma} = 0.0338]	1896 [R_{int} = 0.1124, R_{sigma} = 0.0764]	17196 [R_{int} = 0.0535, R_{sigma} = 0.0625]
Data/restraints/parameters	8486/20/565	1896/29/172	17196/1172/1227
Goodness-of-fit on F^2	1.059	1.061	1.024
Final R indexes [I>=2σ (I)]	R_1 = 0.0363, wR_2 = 0.0787	R_1 = 0.0612, wR_2 = 0.1342	R_1 = 0.0680, wR_2 = 0.1648
Final R indexes [all data]	R_1 = 0.0459, wR_2 = 0.0823	R_1 = 0.1060, wR_2 = 0.1544	R_1 = 0.1197, wR_2 = 0.1907
Largest diff. peak/hole [e.Å^{-3}]	0.19/-0.19	0.14/-0.16	0.47/-0.21
Flack parameter	0.3(4)	-0.8(10)	0.2(7)

Identification code	(*rac*)-BINOL-(*rac*)-DACH-EtOAc *rac-rac*-EtOAc	(*rac*)-Binol-(*rac*)-DACH *rac-rac*	(*rac*)-BINOL-(*rac*)-DACH-MeOH *rac-rac*-MeOH
Empirical formula	$C_{28}H_{32}N_2O_3$	$C_{26}H_{28}N_2O_2$	$C_{27}H_{32}N_2O_3$
Formula weight [g/mol]	444.55	400.50	432.54
Temperature [K]	297(2)	297(2)	297(2)
Crystal system	triclinic	monoclinic	triclinic
Space group	*P*-1	$P2_1/c$	*P*-1
a [Å]	8.1693(10)	8.1707(5)	10.2697(12)
b [Å]	9.2052(9)	29.731(2)	11.140(2)
c [Å]	16.684(2)	9.0449(6)	11.3987(17)
α [°]	96.026(9)	90	108.518(16)
β [°]	95.209(10)	101.667(6)	101.580(12)
γ [°]	102.224(9)	90	101.228(14)
Volume [Å^3]	1211.1(2)	2151.8(3)	1163.6(3)
Z	2	4	2
ρ_{calc} [g/cm^3]	1.219	1.236	1.235
μ [mm^{-1}]	0.079	0.078	0.080
F(000)	476.0	856.0	464.0
Crystal size [mm^3]	0.5 × 0.2 × 0.1	0.15 × 0.1 × 0.05	0.3 × 0.23 × 0.03
Radiation	MoKα (λ = 0.71073)	MoKα (λ = 0.71073)	MoKα (λ = 0.71073)
2Θ range for data collection [°]	5.954 to 53.13	5.354 to 50.51	6.502 to 52.598
Index ranges	-9 ≤ h ≤ 10, -11 ≤ k ≤ 11, -20 ≤ l ≤ 20	-9 ≤ h ≤ 9, -35 ≤ k ≤ 35, -10 ≤ l ≤ 10	-12 ≤ h ≤ 12, -13 ≤ k ≤ 13, -14 ≤ l ≤ 14
Reflections collected	18971	18727	16245
Independent reflections	4925 [R_{int} = 0.0258, R_{sigma} = 0.0188]	3860 [R_{int} = 0.0691, R_{sigma} = 0.0551]	4618 [R_{int} = 0.0364, R_{sigma} = 0.0293]
Data/restraints/parameters	4925/46/343	3860/0/287	4618/224/381
Goodness-of-fit on F^2	1.055	1.124	1.059
Final R indexes [I>=2σ (I)]	R_1 = 0.0454, wR_2 = 0.1183	R_1 = 0.0831, wR_2 = 0.1398	R_1 = 0.0612, wR_2 = 0.1531
Final R indexes [all data]	R_1 = 0.0544, wR_2 = 0.1239	R_1 = 0.1398, wR_2 = 0.1616	R_1 = 0.0793, wR_2 = 0.1624
Largest diff. peak/hole [e.Å^{-3}]	0.19/-0.15	0.17/-0.21	0.22/-0.17

Table SI-2. Hydrogen bonds of the *R-RR* cocrystal (DIFFOO[1]) and labelling of the atoms of interest.

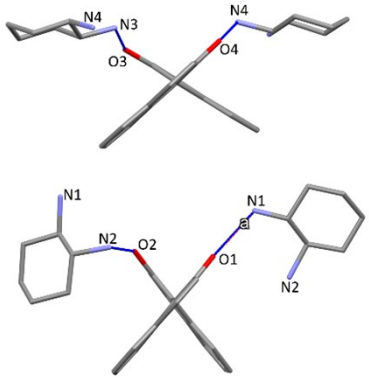

				Interatomic distances (Å)			Angle (°)
Type	Donor	H…	Acceptor	D-H	H…A	D…A	D-H…A
	O1	--H1	..N1	0.82	1.90	2.691(4)	161
	O2	-- H8	.. N2	0.82	2.09	2.796(5)	144

	N2	--H27	..O1	1.04(5)	2.24(5)	3.245(5)	163(4)
Intra	N2	--H27	..N1	1.04(5)	2.56(5)	2.966(6)	103(3)'
	O3	--H29	..N3	0.82	2.00	2.742(4)	151
	O4	--H36	..N4	0.82	2.08	2.808(4)	148

Table SI-3. Hydrogen bonds of the *R-RR*-toluene cocrystal-solvate (SUVNAY[1]).

				Interatomic distances (Å)			Angle (°)
Type	Donor	H…	Acceptor	D-H	H…A	D…A	D-H…A
	O1	--H1	..N1	0.96	2.02	2.7458(4)	131

Table SI-4. CH-π stacking in the *R-RR*-toluene cocrystal-solvate (SUVNAY[1]).

		Distance (Å)	Angle (°)	Interatomic distances (Å)
C-H	Ring	H…Ring	C-H…Ring	C…RingH
C7-H7	Benzene	2.95	175	3.9070(6)
C7-H7	Benzene	2.76	155	3.6519(6)

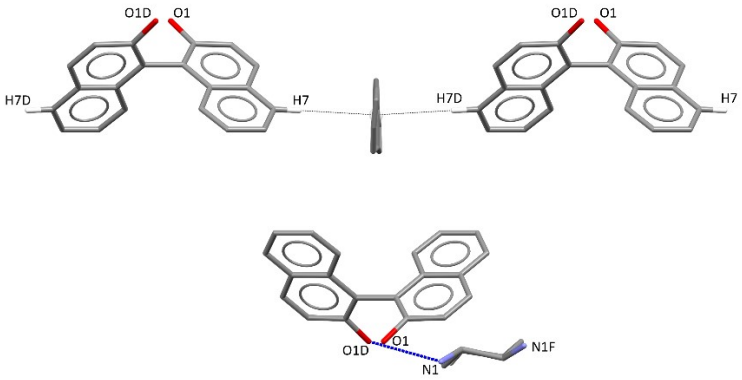

Figure SI-9. CH- π interaction of the *R-RR*-tolu cocrystal-solvate, view along *b*-axis.

Table SI-5. Hydrogen bonds of the *R- RR*-benzene cocrystal-solvate.

				Interatomic distances (Å)			Angle (°)
Type	Donor	H…	Acceptor	D-H	H…A	D…A	D-H…A
	O1	--H1	..N21	0.84(7)	2.00(8)	2.768(7)	151(6)

Table SI-6**.** CH- π stacking in the *R-RR*-benzene cocrystal-solvate, obtained in benzene.

		Distance (Å)	Angle (°)	Interatomic distances (Å)
C-H	Ring	H…Ring	C-H…Ring	C…RingH
C6-H6	Benzene	2.88	169	3.796(8)
C6-H6	Benzene	2.88	169	3.796(8)

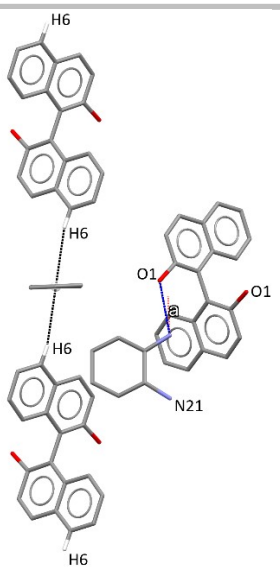

Figure SI-10. CH-π interaction of the *R-RR*-benz cocrystal-solvate, view along *a*-axis.

Table SI-7**.** Hydrogen bonds of the *S-RR* cocrystal (SUVNEC[1]) and labelling of the atoms of interest.

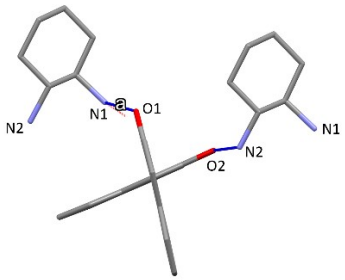

				Interatomic distances (Å)			Angle (°)
Type	Donor	H…	Acceptor	D-H	H…A	D…A	D-H…A
	O1	--H1	..N1	0.96	1.85	2.737(4)	153
	O2	--H2	..N2	0.96	1.88	2.813(5)	164

Table SI-8. Hydrogen bonds of the 4*rac-4RR*-3EtOH-H_2O cocrystal-salt-solvate, obtained in EtOH and labelling of the atoms of interest.

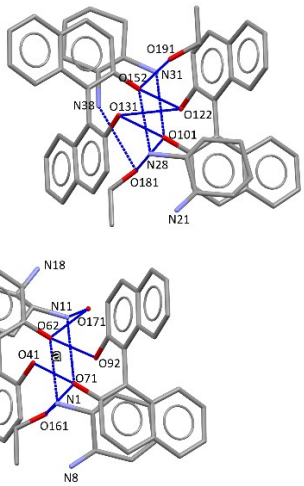

					Interatomic distances (Å)		Angle (°)
Type	Donor	--- H..	..Acceptor	D - H	H...A	D...A	D - H...A

	N1	--H1A	..O62	0.89	1.90	2.792(8)	178
Intra	N1	--H1B	..N8	0.89	2.37	2.787(9)	109
	N1	--H1C	..O161	0.89	1.85	2.735(8)	176
Intra	N11	--H11A	..N18	0.89	2.34	2.798(11)	112
	N11	--H11B	..O71	0.89	1.98	2.862(8)	173
	N11	--H11C	..O171	0.89	1.90	2.759(9)	160
Intra	N21	--H21A	..N28	0.89(4)	2.52(10)	2.815(13)	100(7)
	N28	--H28A	..O152	0.89	1.90	2.785(8)	172
Intra	N28	--H28B	..N21	0.89	2.37	2.815(13)	111
	N28	--H28C	..O181	0.89	1.92	2.807(10)	172
	N31	--H31B	..O101	0.89	1.93	2.816(8)	170
	N31	--H31C	..O191	0.89	1.85	2.719(9)	164
	N38	--H38B	..O131	0.89(9)	2.42(9)	3.270(14)	162(6)
	O41	--H41	..O71	0.82	1.83	2.620(7)	161
	O171	--H71B	..O62	0.91(8)	1.82(9)	2.702(8)	162(7)
	O92	--H92	..O62	0.82	1.87	2.613(7)	150
	O122	--H122	..O152	0.82	1.85	2.628(7)	157
	O131	--H131	..O101	0.82	1.87	2.612(7)	150
	O161	--H161	..O71	0.82	1.78	2.601(7)	174
	O181	--H181	..O101	0.82	1.91	2.680(9)	157
	O191	--H183	..O152	0.82	1.85	2.636(8)	160

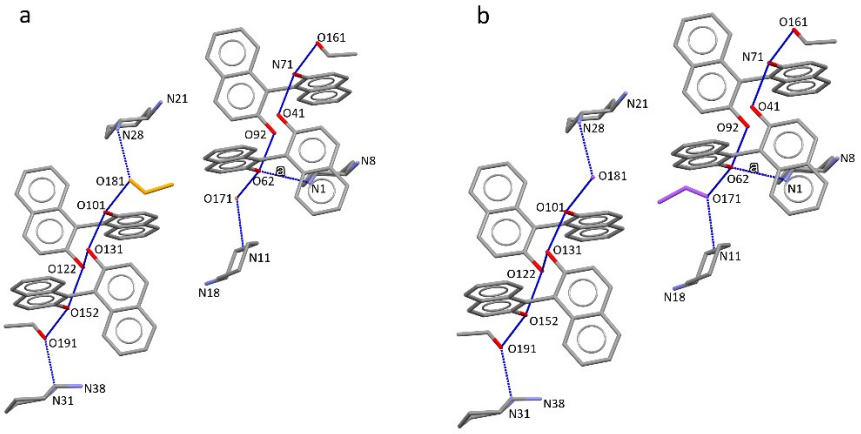

Figure SI-11. 4*rac-4RR*-3EtOH-H_2O phase, view along b-axis. Of the three molecules of EtOH, one is disordered, the molecule of water is also disordered. The disordered molecule of EtOH and the molecule of water can be exchanged, with the major form accounting for 67.8% and the minor form for 32.2%. a) Major form, in orange, b) Minor form, in blue.

Table SI-9**.** Hydrogen bonds of the *rac-rac*-MeOH cocrystal-salt-solvate obtained in MeOH.

				Interatomic distances (Å)			Angle (°)
Type	Donor	H…	Acceptor	D-H	H…A	D…A	D-H…A
	O22	--H22	..O1	0.97(3)	1.68(3)	2.617(2)	162(2)
Intra	N31	--H31A	..N38	0.89	2.38	2.798(15)	109
	N31	--H31A	..N38B	0.89	2.39	2.820(19)	110’
	N31	--H31B	..O1	0.89	1.81	2.690(14)	171
	N31	--H31C	..O41	0.89	2.01	2.891(16)	172
	O41	--H41	..O1	0.98(3)	1.69(3)	2.656(3)	173(3)

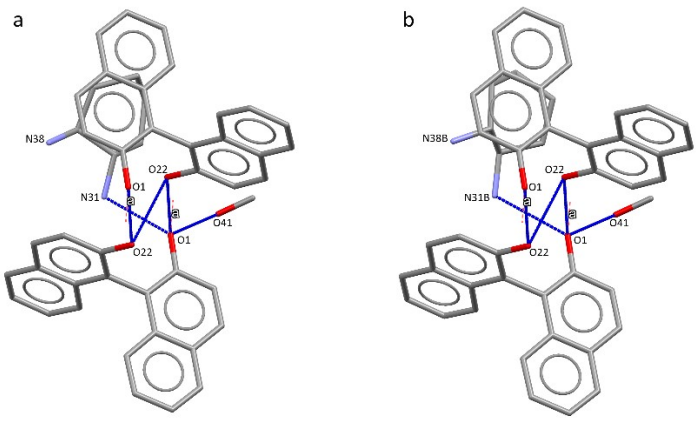

Figure SI-12. *rac-rac*-MeOH phase, view along a-axis. DACH molecule shows S-*R* disorder, as 51%-49%. a) Major form, b) Minor form.

Table SI-10**.** Hydrogen bonds of the *rac-rac*-EtOAc cocrystal-solvate, obtained by slow evaporation and labelling of the atoms of interest.

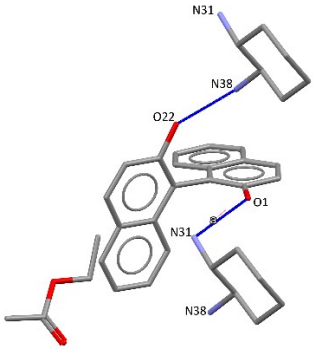

				Interatomic distances (Å)			Angle (°)
Type	Donor	H…	Acceptor	D-H	H…A	D…A	D-H…A
	O1	--H1	..N31	0.91(2)	1.96(2)	2.815(2)	154.8(15)
	O22	--H22	..N38	0.96(2)	1.911(17)	2.763(2)	146.9(13)

Table SI-11**.** Hydrogen bonds of the *rac-rac* cocrystal obtained in ACN and labelling of the atoms of interest.

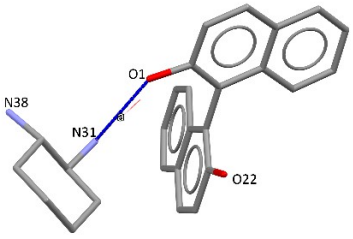

				Interatomic distances (Å)			Angle (°)
Type	Donor	H…	..Acceptor	D - H	H...A	D...A	D - H...A
	O1	--H1	..N31	0.88(3)	1.98(3)	2.786(4)	152(2)
	O22	--H22	..N38	0.94(3)	1.98(3)	2.842(4)	152(3)

Thermogravimetric analysis

TGA

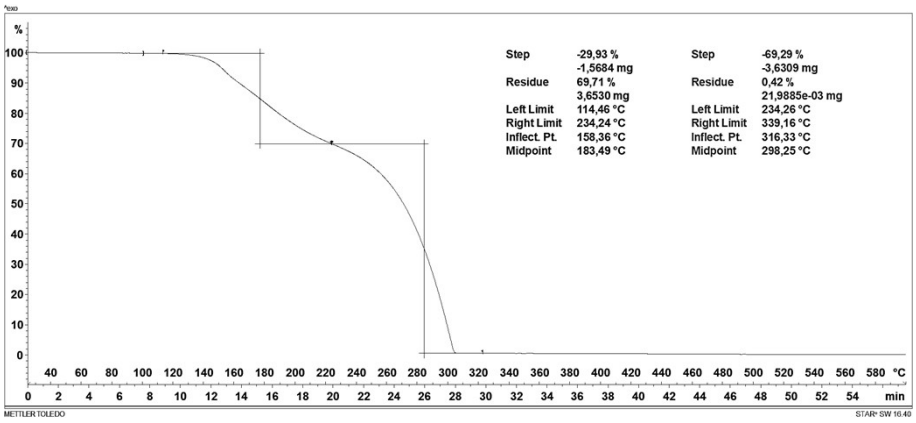

Figure SI-13. TGA of the *R-RR* (1:1) cocrystal, obtained by slurrying (*R*)-BINOL and (*R,R*)-DACH in a 1:1 ratio in MeOH. The thermogram is expressed as the weight loss (%) with respect to temperature. It shows a two-step mass loss starting at 114°C, consisting in the degradation of the product.

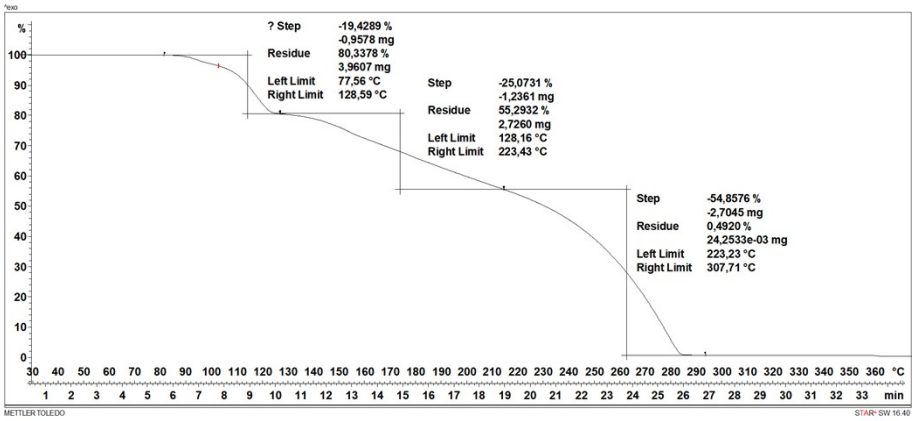

Figure SI-14. TGA of the *R-RR*-tolu (1:1:1) cocrystal-solvate, obtained by slurrying (*R*)-BINOL and (*R,R*)-DACH in a 1:1 ratio in toluene. The thermogram is expressed as the weight loss (%) with respect to temperature. It shows a three-step mass loss. The first one (starting at 78°C) consists in the drying of the powder and desolvation of toluene (loss of 1 equivalent of toluene), the second (starting at 128°C) and third (starting at 223°C) consist in the degradation of the *R-RR* compound.

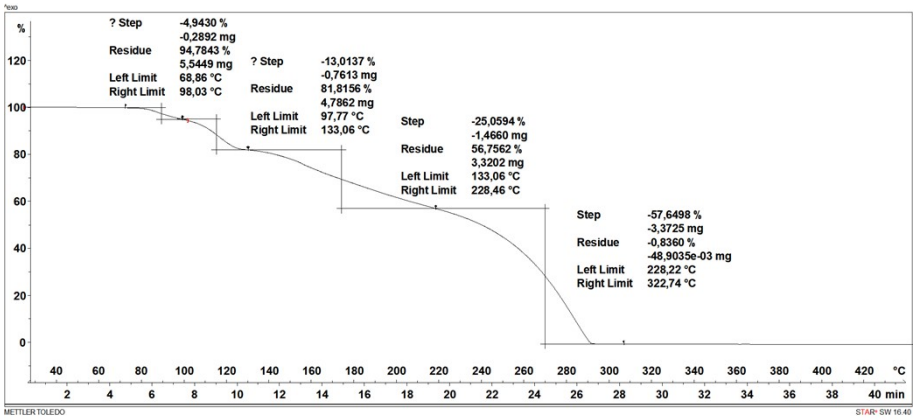

Figure SI-15. TGA of the *R-RR*-benz (1:1:1) cocrystal-solvate, obtained by slurrying (*R*)-BINOL and (*R,R*)-DACH in a 1:1 ratio in benzene. The thermogram is expressed as the weight loss (%) with respect to temperature. It shows a four-step mass loss. The two first ones (starting at 69°C) consist in the desolvation of benzene (loss of 1.1 equivalent of benzene), the third (starting at 133°C) and fourth (starting at 228°C) consist in the degradation of the *R-RR* compound.

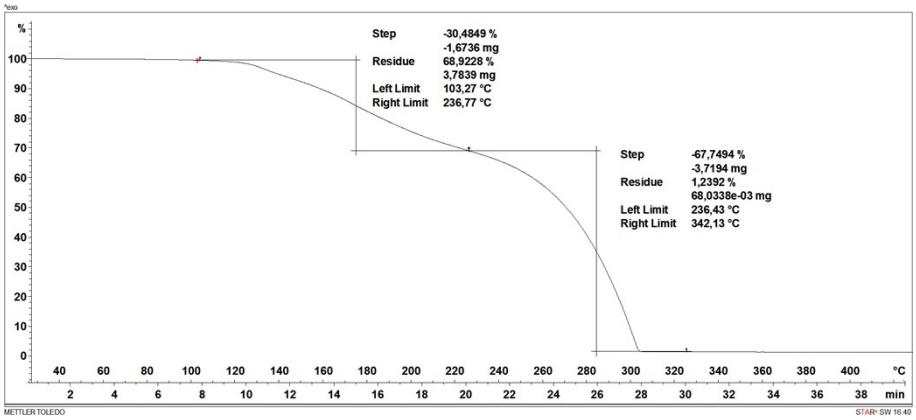

Figure SI-16**.** TGA of the *S-RR* (1:1) cocrystal, obtained by slurrying (*S*)-BINOL and (*R,R*)-DACH in a 1:1 ratio in EtOAc. The thermogram is expressed as the weight loss (%) with respect to temperature. It shows a two-step mass loss starting at 64°C, consisting in the degradation of the product.

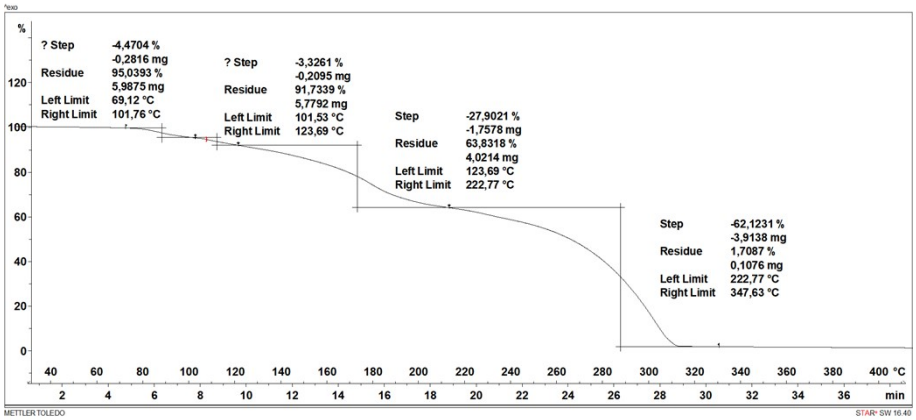

Figure SI-17. TGA of the *rac-RR*-MeOH (1:1:1) phase, obtained by slurrying (*rac*)-BINOL and (*R,R*)-DACH in a 1:1 ratio in MeOH. The thermogram is expressed as the weight loss (%) with respect to temperature. It shows a four-step mass loss. The two first ones (starting at 69°C) consist in the desolvation of methanol (loss of 1.1 equivalent of MeOH), the third (starting at 124°C) and fourth (starting at 223°C) consist in the degradation of the *rac-RR* compound.

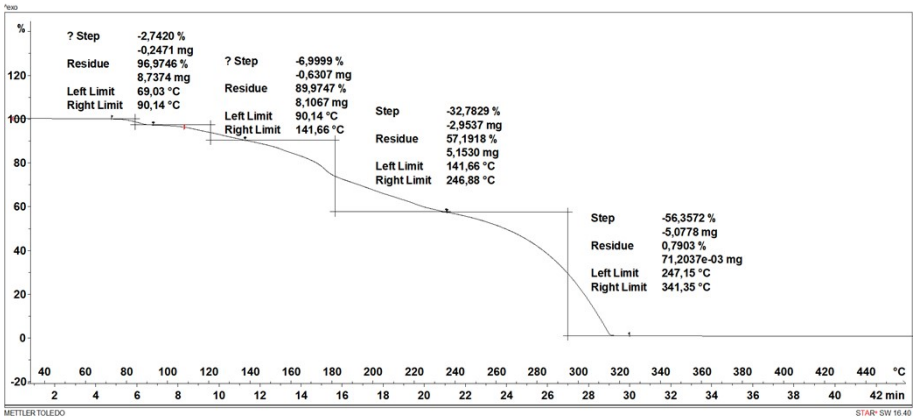

Figure SI-18**.** TGA of the 4*rac-4RR*-3EtOH-H_2O (4:4:3:1) phase, obtained by slurrying (*rac*)-BINOL and (*R,R*)-DACH in a 1:1 ratio in EtOH. The thermogram is expressed as the weight loss (%) with respect to temperature. It shows a four-step mass loss. The two first ones (starting at 69°C) consist in the desolvation of ethanol and water, the third (starting at 142°C) and fourth (starting at 247°C) consist in the degradation of the *rac-RR* compound.

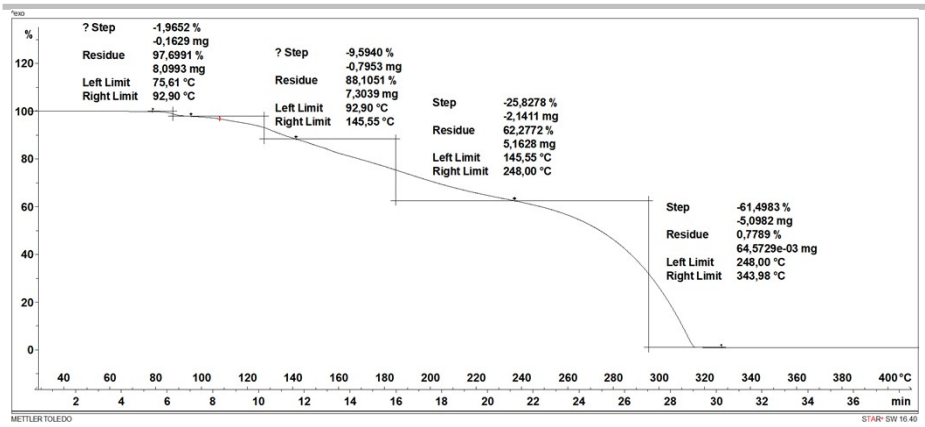

Figure SI-19**.** TGA of the new form, obtained by slurrying (*rac*)-BINOL and (*R,R*)-DACH in a 1:1 ratio in EtOAc. The thermogram is expressed as the weight loss (%) with respect to temperature. It shows a four-step mass loss. The two first ones (starting at 77°C) consist in the desolvation of ethyl acetate (loss of 0.6 equivalent of EtOAc), the third (starting at 170°C) and fourth (starting at 250°C) consist in the degradation of the *rac-RR* compound.

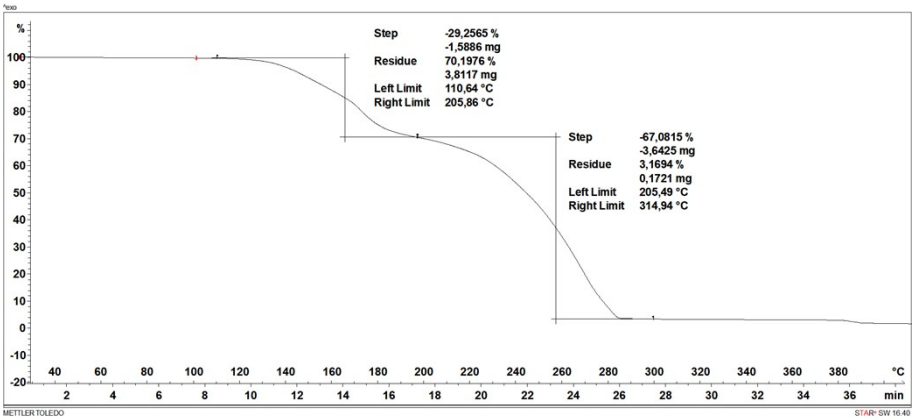

Figure SI-20**.** TGA of the newly crystal phase, obtained by slurrying (*rac*)-BINOL and (*rac*)-DACH in a 1:1 ratio in EtOAc. The thermogram is expressed as the weight loss (%) with respect to temperature. It shows a two-step mass loss starting at 111°C, consisting in the degradation of the product.

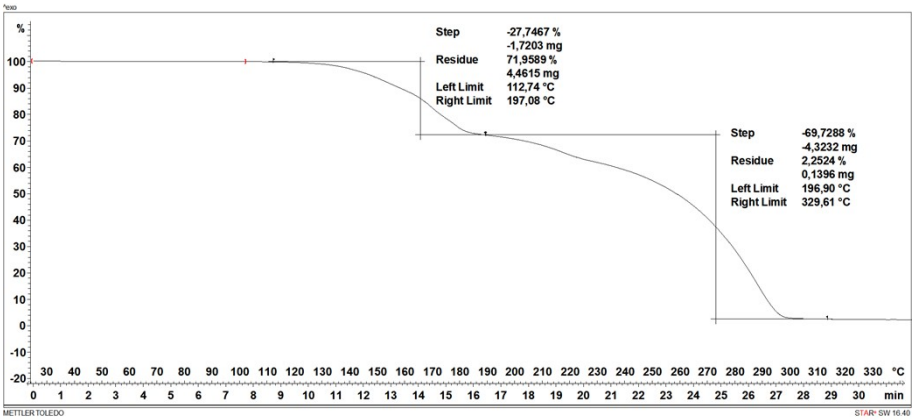

Figure SI-21**.** TGA of the *rac-rac* (1:1) phase, obtained by slurrying (*rac*)-BINOL and (*rac*)-DACH in a 1:1 ratio in ACN. The thermogram is expressed as the weight loss (%) with respect to temperature. It shows a two-step mass loss starting at 113°C, consisting in the degradation of the product.

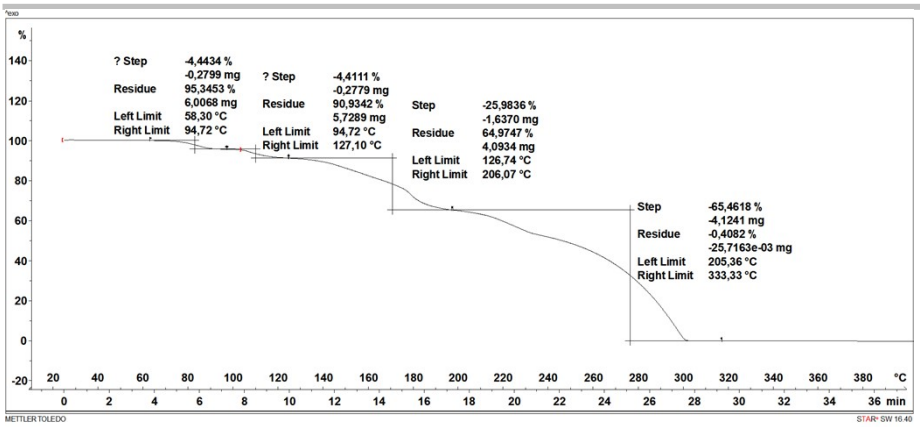

Figure SI-22**.** TGA of the *rac-rac*-MeOH (1:1:1) phase, obtained by slurrying (*rac*)-BINOL and (*rac*)-DACH in a 1:1 ratio in MeOH. The thermogram is expressed as the weight loss (%) with respect to temperature. It shows a four-step mass loss. The two first ones (starting at 58°C) consist in the desolvation of methanol (loss of 1.2 equivalent of MeOH), the third (starting at 127°C) and fourth (starting at 205°C) consist in the degradation of the *rac-rac* compound.

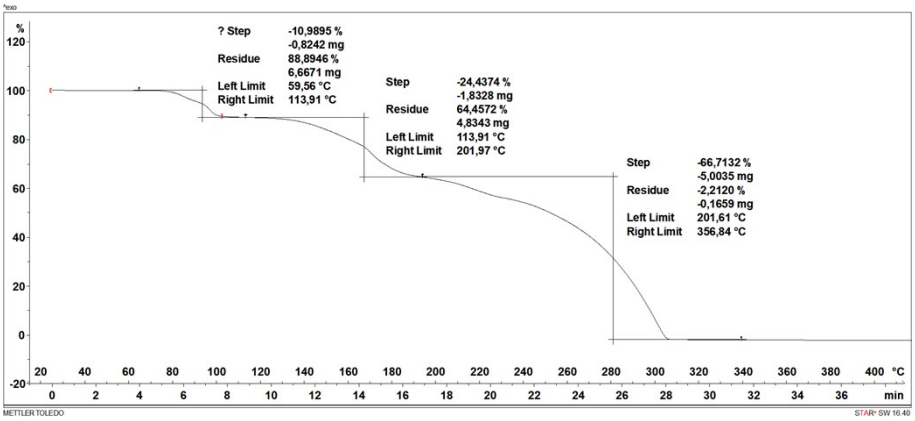

Figure SI-23**.** TGA of the newly crystal phase, obtained by slurrying (*rac*)-BINOL and (*rac*)-DACH in a 1:1 ratio in EtOH. The thermogram is expressed as the weight loss (%) with respect to temperature. It shows a three-step mass loss. The first one (starting at 60°C) consists in the desolvation of ethanol (loss of 1 equivalent of EtOH), the second (starting at 114°C) and third (starting at 202°C) consist in the degradation of the *rac-rac* compound.

DSC

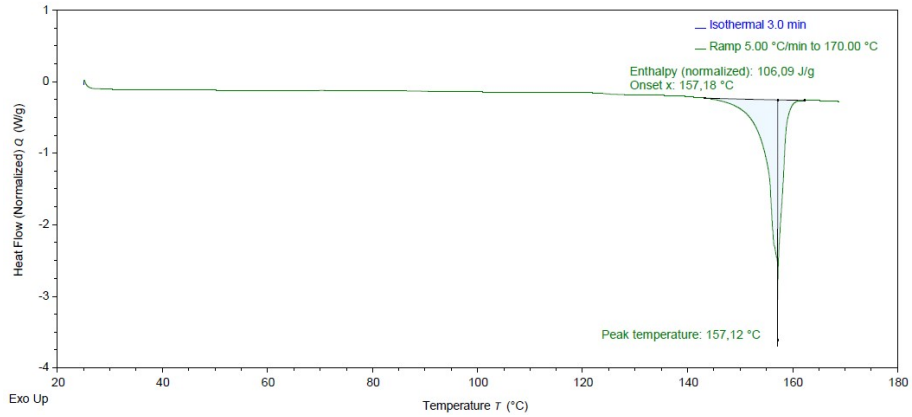

Figure SI-24**.** DSC of the *R-RR* (1:1) cocrystal, obtained by slurrying (*R*)-BINOL and (*R,R*)-DACH in a 1:1 ratio in EtOH. The thermogram is expressed as the heat flow (Q) with respect to temperature. It shows one peak (157°C) consisting of the melting of the compound.

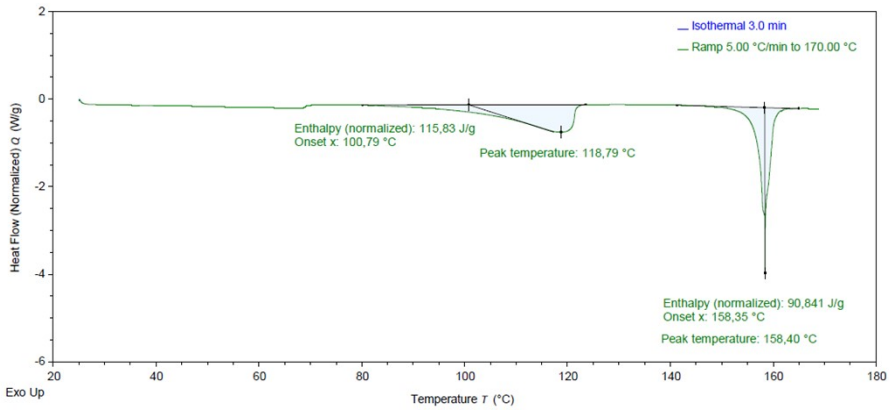

Figure SI-25**.** DSC of the *R-RR*-tolu (1:1:1) cocrystal-solvate, obtained by slurrying (*R*)-BINOL and (*R,R*)-DACH in a 1:1 ratio in toluene. The thermogram is expressed as the heat flow (Q) with respect to temperature. It shows two peaks. The first one (with an onset of 101°C) corresponds to the desolvation of toluene, the second one (with an onset of 158°C) consists of the melting of the *R-RR* compound.

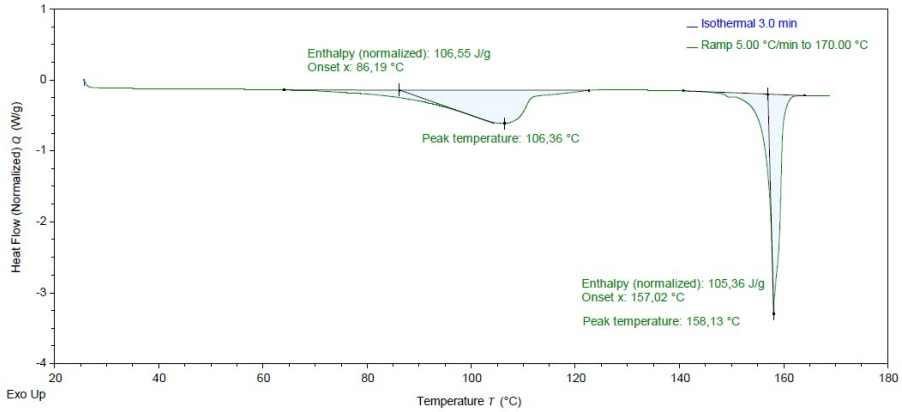

Figure SI-26**.** DSC of the *R-RR*-benz (1:1:1) cocrystal-solvate, obtained by slurrying (*R*)-BINOL and (*R,R*)-DACH in a 1:1 ratio in benzene. The thermogram is expressed as the heat flow (Q) with respect to temperature. It shows two peaks. The first one (with an onset of 86°C) corresponds to the desolvation of benzene, the second one (with an onset of 158°C) consists of the melting of the *R-RR* compound.

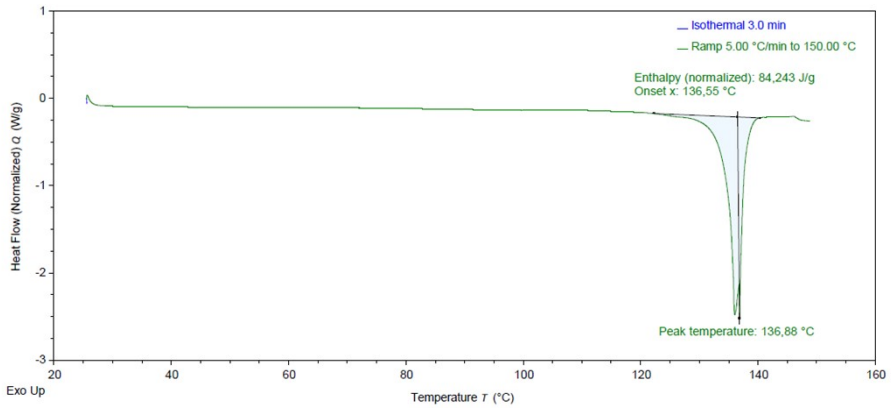

Figure SI-27**.** DSC of the *S-RR* (1:1) cocrystal, obtained by slurrying (*S*)-BINOL and (*R,R*)-DACH in a 1:1 ratio in EtOAc. The thermogram is expressed as the heat flow (Q) with respect to temperature. It shows one peak (with an onset of 137°C) consisting in the melting of the compound.

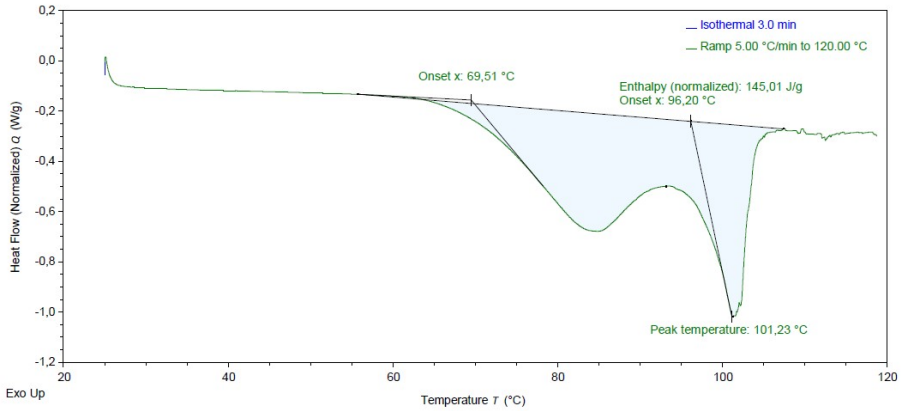

Figure SI-28**.** DSC of the *rac*-*RR*-MeOH material, obtained by slurrying (*rac*)-BINOL and (*R,R*)-DACH in a 1:1 ratio in MeOH. The thermogram is expressed as the heat flow (Q) with respect to temperature. It shows two peaks (with onsets of respectively 70°C and 96°C), the first one consists of the desolvation of methanol and the second consists of the melting of the *rac*-*RR* compound.

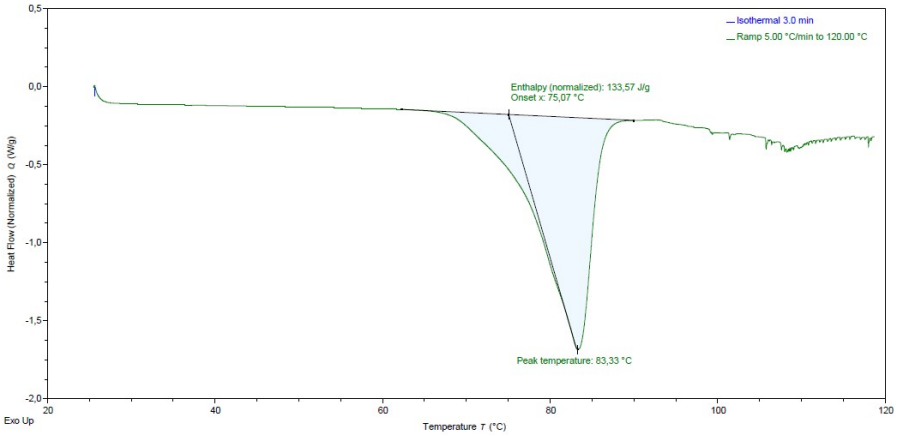

Figure SI-29**.** DSC of the 4*rac*-4*RR*-3EtOH-H_2O material, obtained by slurrying (*rac*)-BINOL and (*R,R*)-DACH in a 1:1 ratio in EtOH. The thermogram is expressed as the heat flow (Q) with respect to temperature. It shows one shouldered peak (with an onset of 75°C), consisting of the desolvation and melting of the compound, before its degradation.

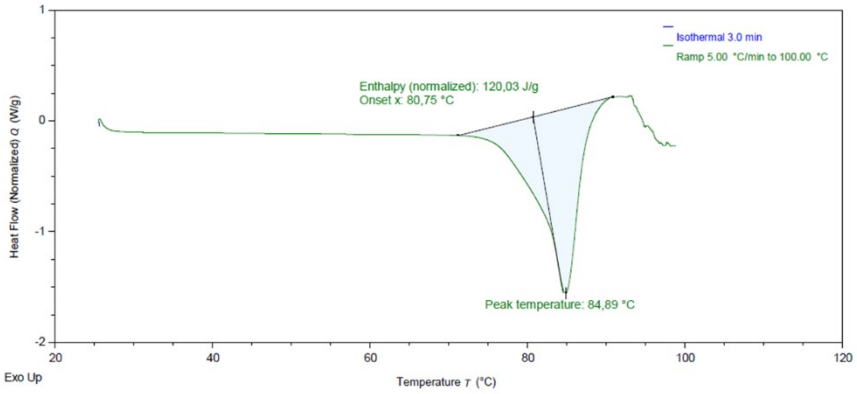

Figure SI-30**.** DSC of the material obtained by slurrying (*rac*)-BINOL and (*R,R*)-DACH in a 1:1 ratio in EtOAc. The thermogram is expressed as the heat flow (Q) with respect to temperature. It shows one shouldered peak (with an onset of 81°C), consisting of the desolvation and melting of the compound, before its degradation.

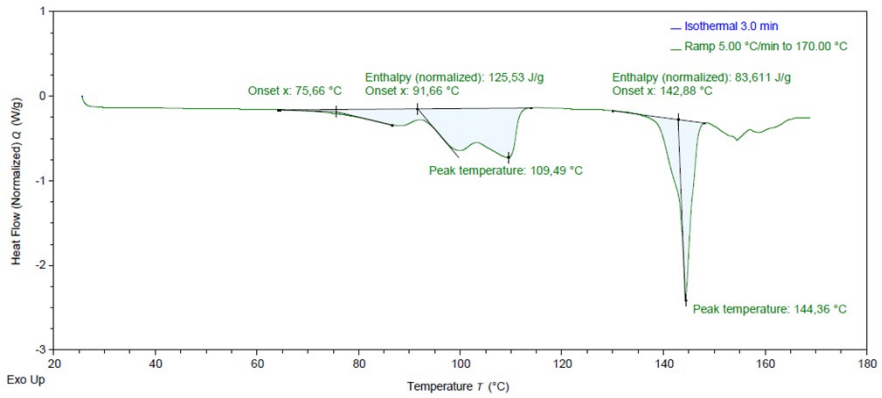

Figure SI-31. DSC of the material obtained by slurrying (*rac*)-BINOL and (*rac*)-DACH in a 1:1 ratio in toluene. The thermogram is expressed as the heat flow (Q) with respect to temperature. It shows three shouldered peaks (with an onset of 76°C), consisting of the drying and desolvation of the compound, before its melting (characterized by a peak with an onset of 143°C) and its degradation.

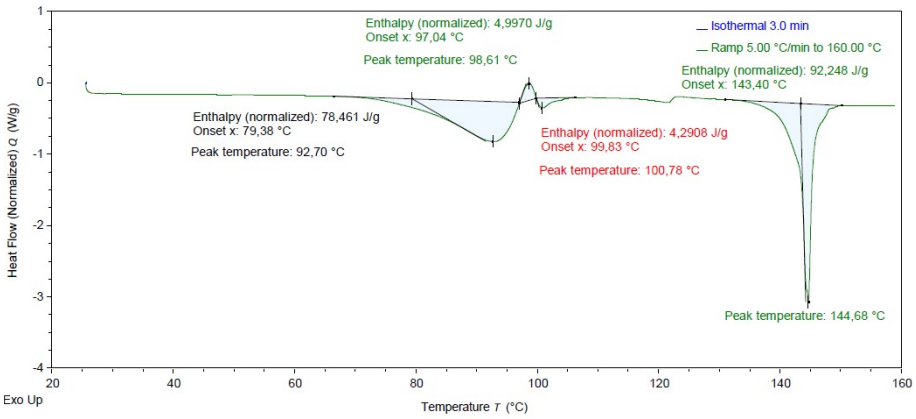

Figure SI-32. DSC of the material obtained by slurrying (*rac*)-BINOL and (*rac*)-DACH in a 1:1 ratio in benzene. The thermogram is expressed as the heat flow (Q) with respect to temperature. It shows different events. The first event (with an onset of 79°C) corresponds to the desolvation of benzene, The final compound melts melts at 143°C.

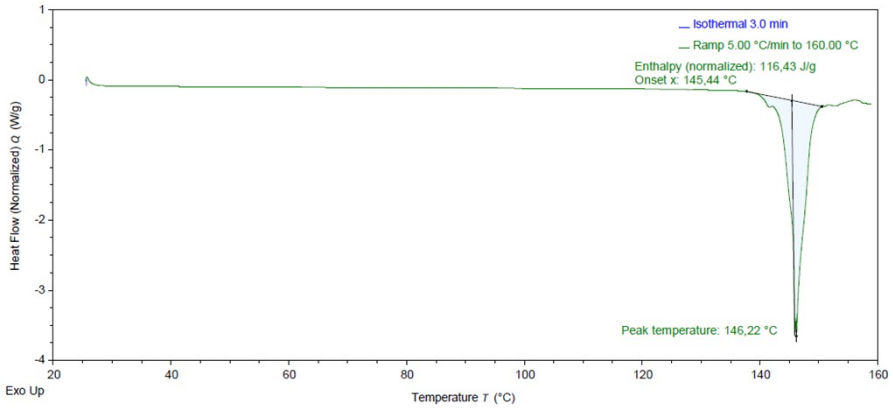

Figure SI-33**.** DSC of the material obtained by slurrying (*rac*)-BINOL and (*rac*)-DACH in a 1:1 ratio in EtOAc. The thermogram is expressed as the heat flow (Q) with respect to temperature. It shows one peak (with an onset of 145°C) consisting of the melting of the compound.

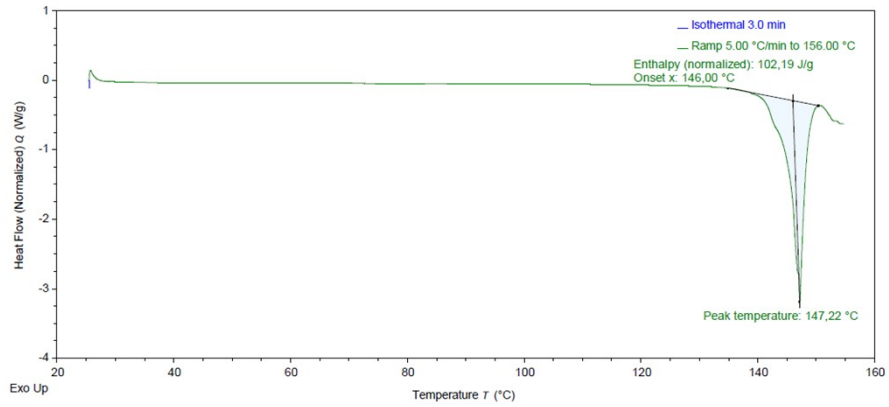

Figure SI-34**.** DSC of the *rac-rac* cocrystal obtained by slurrying (*rac*)-BINOL and (*rac*)-DACH in a 1:1 ratio in ACN. The thermogram is expressed as the heat flow (Q) with respect to temperature. It shows one peak (with an onset of 146°C) consisting of the melting of the compound.

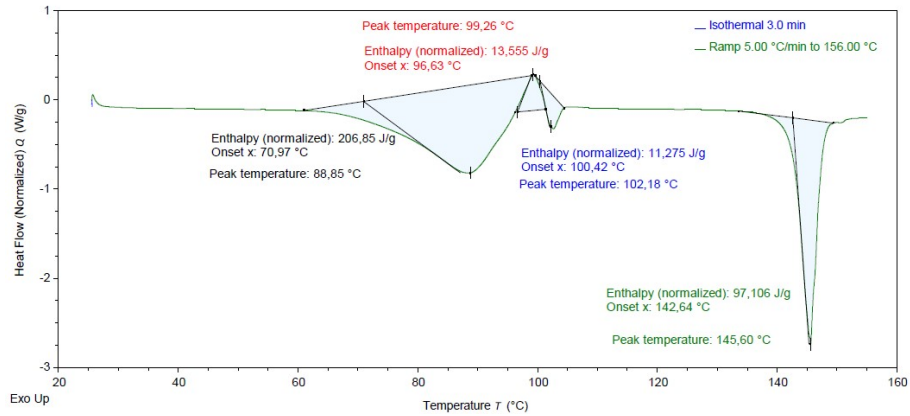

Figure SI-35**.** DSC of the *rac-rac*-MeOH compound obtained by slurrying (*rac*)-BINOL and (*rac*)-DACH in a 1:1 ratio in MeOH. The thermogram is expressed as the heat flow (Q) with respect to temperature. It shows different events. The first peak (with an onset of 71°C) corresponds to a desolvation event. The final *rac-rac* compound melts (characterized by a peak with an onset of 143°C).

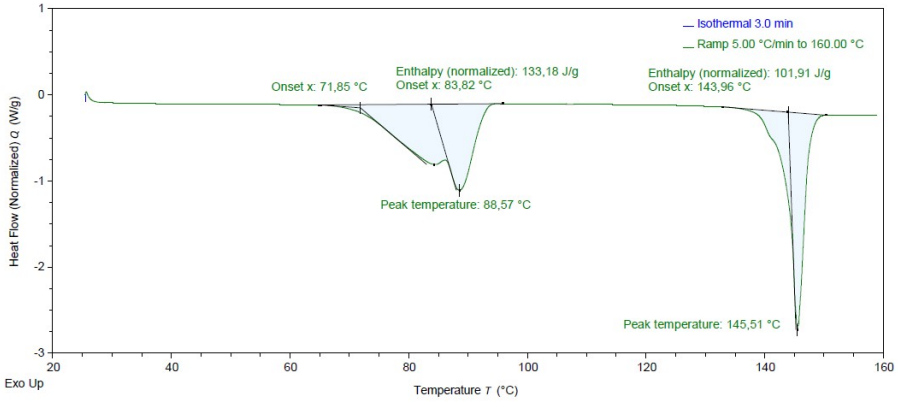

Figure SI-36**.** DSC of the material obtained by slurrying (*rac*)-BINOL and (*rac*)-DACH in a 1:1 ratio in EtOH. The thermogram is expressed as the heat flow (Q) with respect to temperature. It shows two shouldered peaks (with an onset of 72°C), consisting of the desolvation of ethanol, followed by an endothermic peak (with an onset of 144°C) consisting of the melting of the *rac-rac* compound.

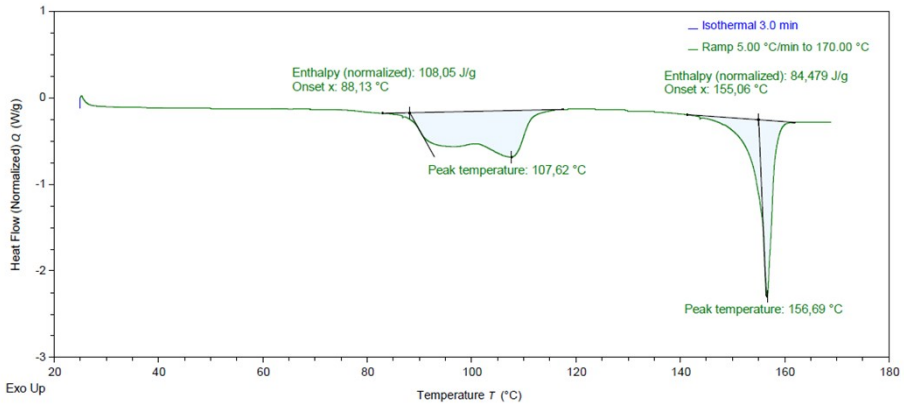

Figure SI-37. DSC of the *R-RR*-tolu compound obtained by slurrying (*R*)-BINOL and (*rac*)-DACH in a 1:1 ratio in toluene. The thermogram is expressed as the heat flow (Q) with respect to temperature. It shows two shouldered peaks (with an onset of 88°C), consisting of the desolvation of the toluene, followed by an endothermic peak (with an onset of 155°C) consisting of the melting of the *R-RR* compound.

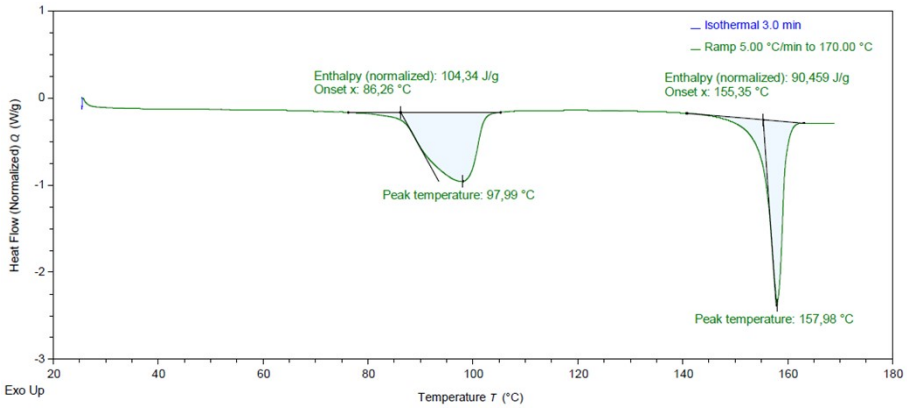

Figure SI-38. DSC of the *R-RR*-benz compound obtained by slurrying (*R*)-BINOL and (*rac*)-DACH in a 1:1 ratio in benzene. The thermogram is expressed as the heat flow (Q) with respect to temperature. It shows one broad peak (with an onset of 86°C), consisting of the desolvation of the benzene, followed by an endothermic peak (with an onset of 155°C) consisting of the melting of the *R-RR* compound.

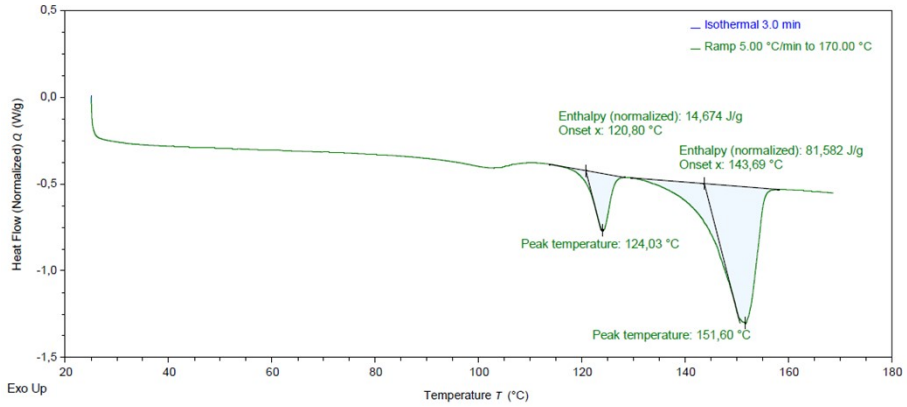

Figure SI-39. DSC of the compound obtained by slurrying (*R*)-BINOL and (*rac*)-DACH in a 1:1 ratio in EtOAc. The thermogram is expressed as the heat flow (Q) with respect to temperature. It shows a eutectic at 121°C followed by a liquidus.

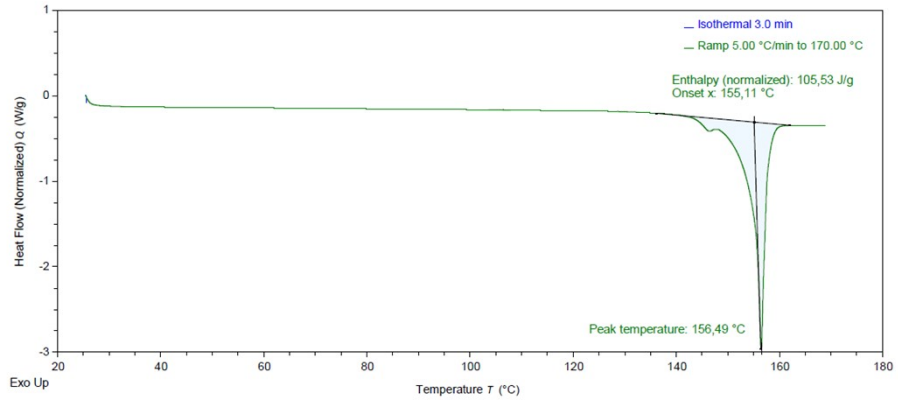

Figure SI-40. DSC of the *R-RR* compound obtained by slurrying (*R*)-BINOL and (*rac*)-DACH in a 1:1 ratio in ACN. The thermogram is expressed as the heat flow (Q) with respect to temperature. It shows one peak (with an onset of 155°C), consisting in the melting of the *R-RR* compound.

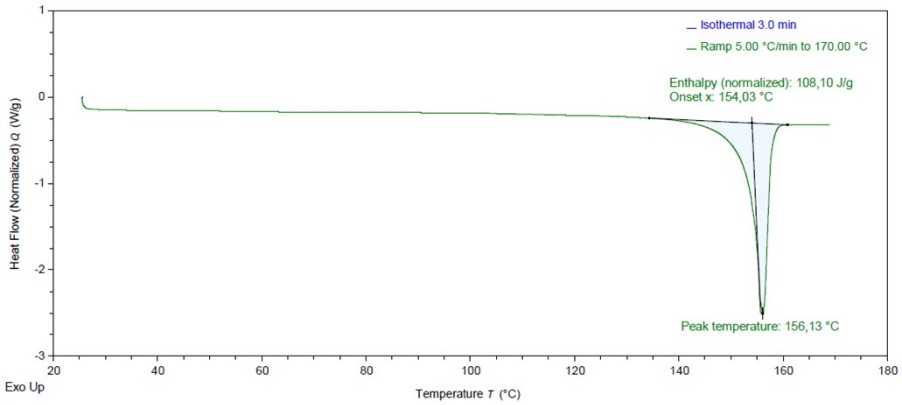

Figure SI-41. DSC of the *R-RR* compound obtained by slurrying (*R*)-BINOL and (*rac*)-DACH in a 1:1 ratio in MeOH. The thermogram is expressed as the heat flow (Q) with respect to temperature. It shows one peak (with an onset of 155°C), consisting in the melting of the *R-RR* compound.

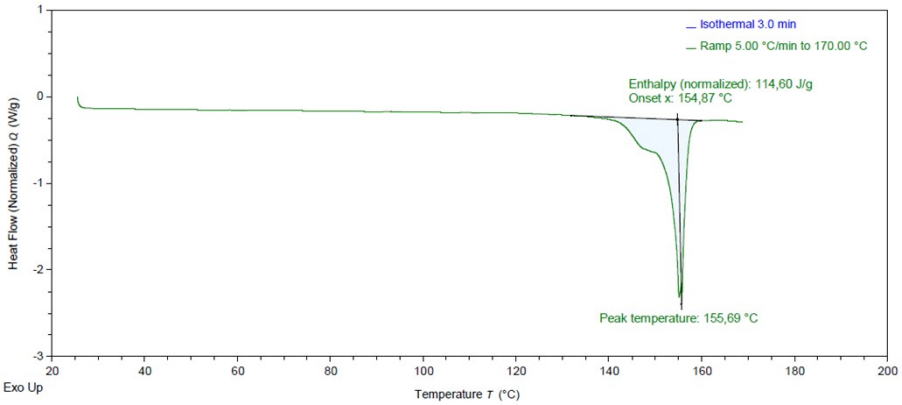

Figure SI-42. DSC of the *R-RR* compound obtained by slurrying (*R*)-BINOL and (*rac*)-DACH in a 1:1 ratio in EtOH. The thermogram is expressed as the heat flow (Q) with respect to temperature. It shows one peak (with an onset of 155°C), consisting of the melting of the *R-RR* compound.

NMR

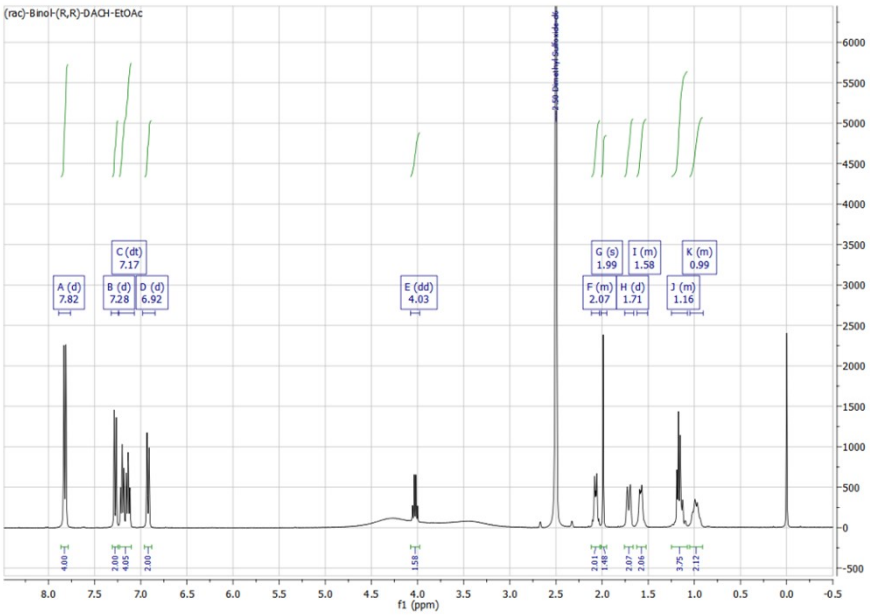

Figure SI-43. ^{1}H NRM of the newly crystal phase, obtained by slurrying (*rac*)-BINOL and (*R,R*)-DACH in a 1:1 ratio in EtOAc. The analysis shows a phase composed by 1 equivalent of BINOL, 1 equivalent of DACH and 0.5 equivalent of EtOAc.

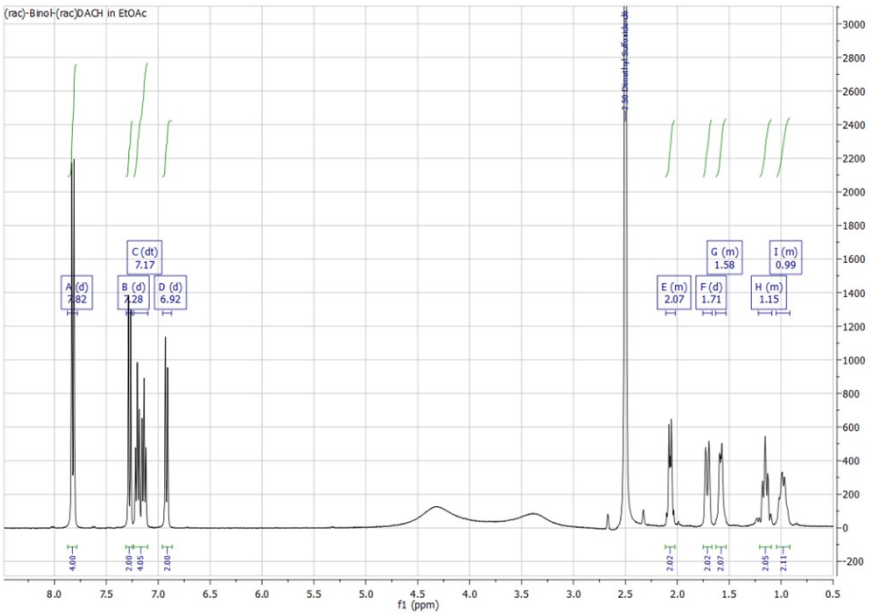

Figure SI-44. ^{1}H NRM of the newly crystal phase, obtained by slurrying (*rac*)-BINOL and (*rac*)-DACH in a 1:1 ratio in EtOAc. The analysis shows a phase composed by 1 equivalent of BINOL and 1 equivalent of DACH.

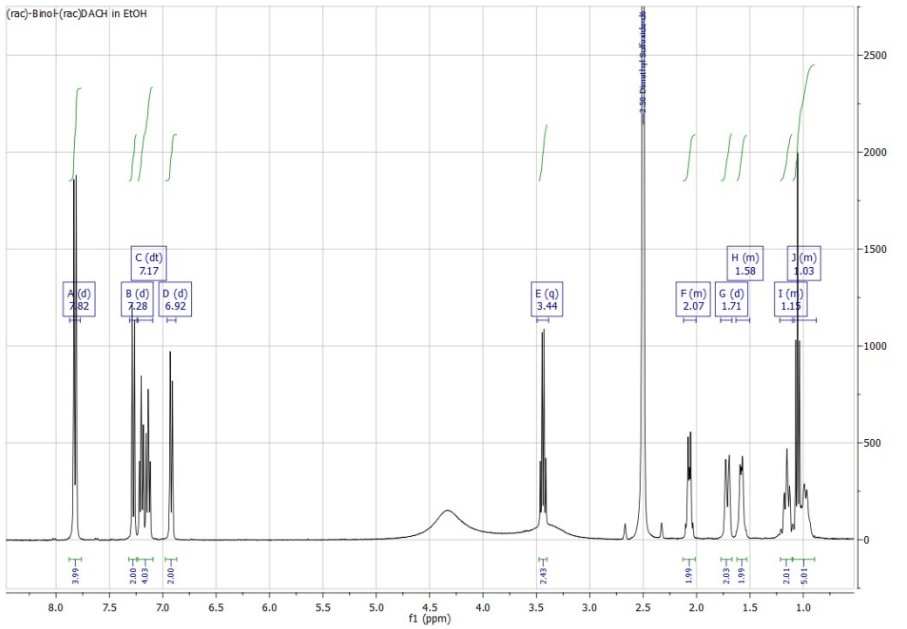

Figure SI-45. ^{1}H NRM of the newly crystal phase, obtained by slurrying (*rac*)-BINOL and (*rac*)-DACH in a 1:1 ratio in EtOH. The analysis shows a phase composed by 1 equivalent of BINOL, 1 equivalent of DACH and 1 equivalent of EtOH.

cHPLC

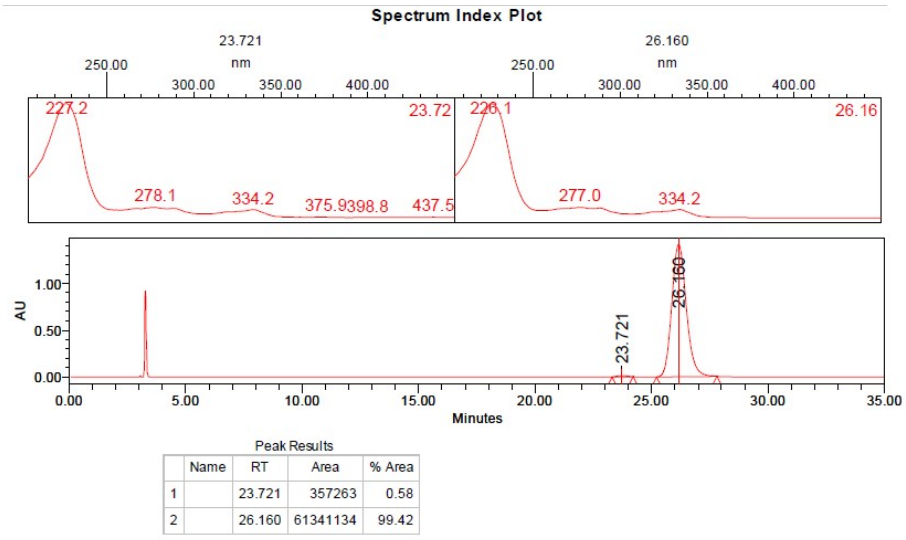

Peak Results

	Name	RT	Area	% Area
1		23.721	357263	0.58
2		26.160	61341134	99.42

Figure SI-46. *c*HPLC analysis of the powder recovered from the resolution of (*rac*)-BINOL by (*R,R*)-DACH in toluene. The first peak corresponds to (*S*)-BINOL and the second to (*R*)-BINOL.

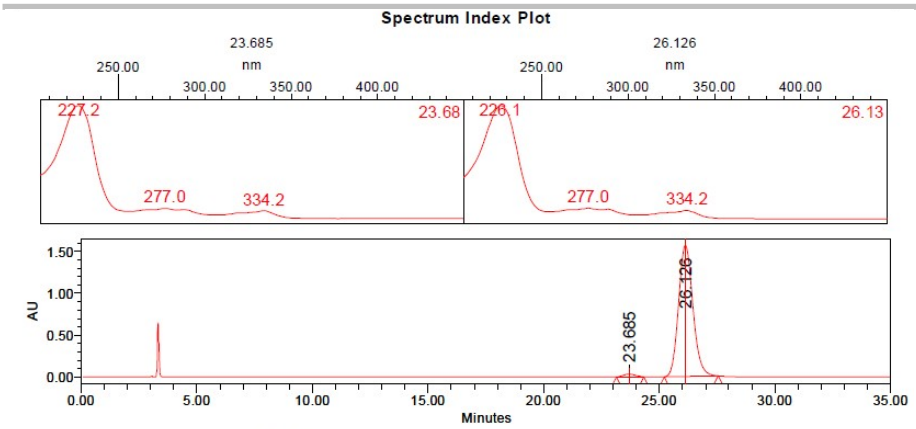

Peak Results

	Name	RT	Area	% Area
1		23.685	1133910	1.64
2		26.126	67811586	98.36

Figure SI-47. *c*HPLC analysis of the powder recovered from the resolution of (*rac*)-BINOL by (*R,R*)-DACH in benzene. The first peak corresponds to (*S*)-BINOL and the second to (*R*)-BINOL.

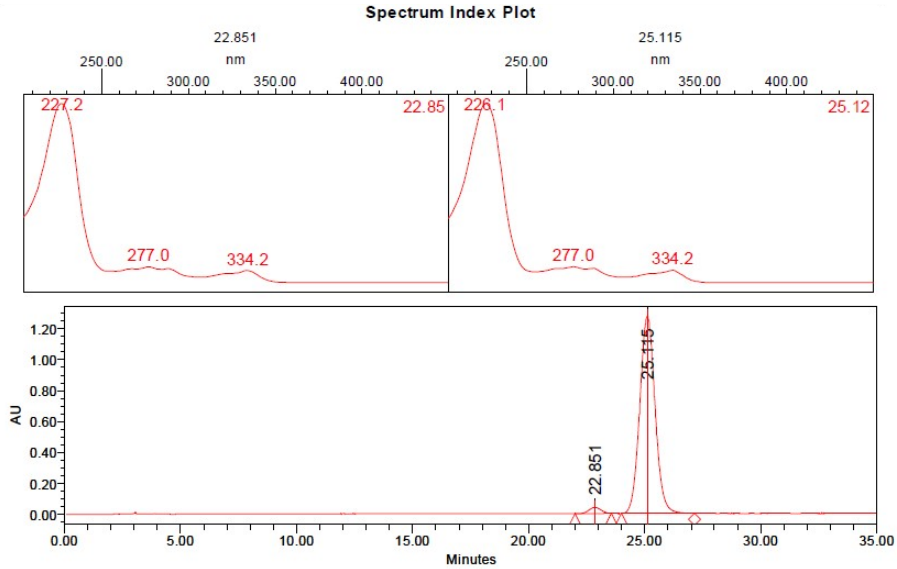

Peak Results

	Name	RT	Area	% Area
1		22.851	1348056	2.28
2		25.115	57898025	97.72

Figure SI-48. *c*HPLC analysis of the powder recovered from the resolution of (*rac*)-BINOL by (*R,R*)-DACH in ACN. The first peak corresponds to (*S*)-BINOL and the second to (*R*)-BINOL.

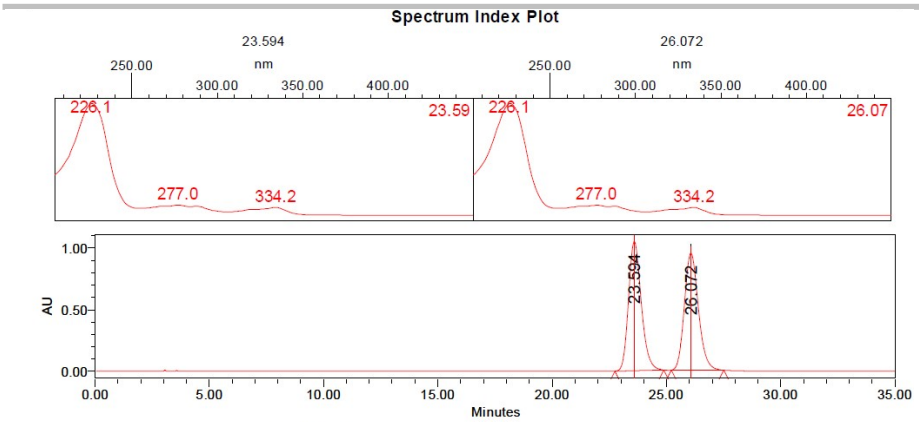

Peak Results

	Name	RT	Area	% Area
1		23.594	40957074	50.17
2		26.072	40681195	49.83

Figure SI-49. *c*HPLC analysis of the newly crystal phase, obtained by slurrying (*rac*)-BINOL and (*rac*)-DACH in a 1:1 ratio in EtOAc. The first peak corresponds to (*S*)-BINOL and the second to (*R*)-BINOL.

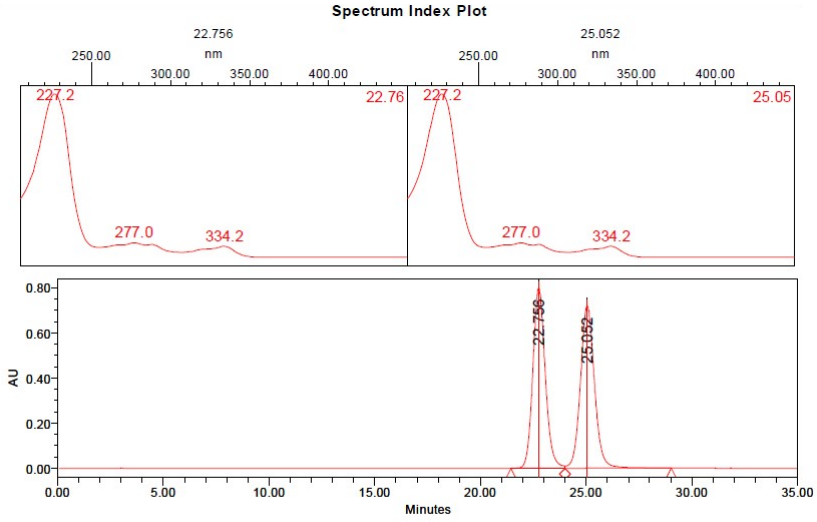

Peak Results

	Name	RT	Area	% Area
1		22.756	32312864	49.48
2		25.052	32998280	50.52

Figure SI-50. *c*HPLC analysis of the newly crystal phase, obtained by slurrying (*rac*)-BINOL and (*R,R*)-DACH in a 1:1 ratio in EtOAc. The first peak corresponds to (*S*)-BINOL and the second to (*R*)-BINOL.

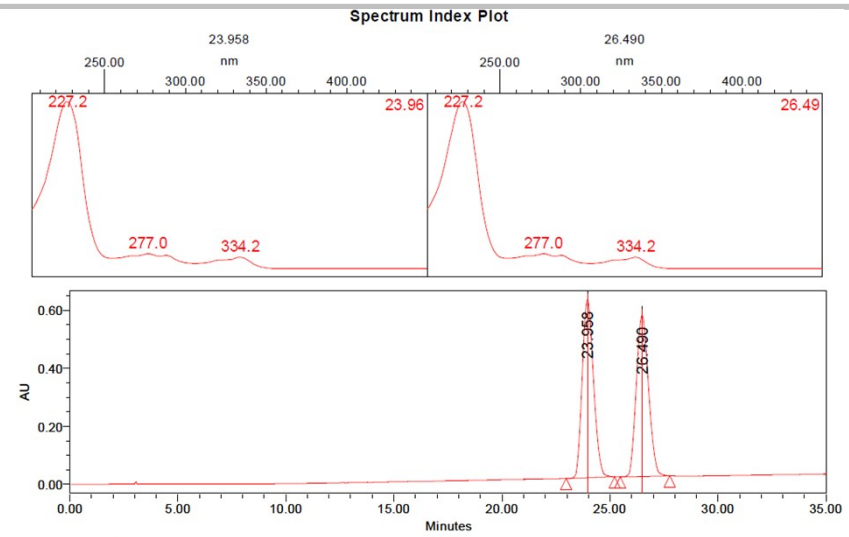

Peak Results

	Name	RT	Area	% Area
1		23.958	22488158	50.45
2		26.490	22085534	49.55

Figure SI-51. *c*HPLC analysis of the newly crystal phase, obtained by slurrying (*rac*)-BINOL and (*rac*)-DACH in a 1:1 ratio in EtOH. The first peak corresponds to (*S*)-BINOL and the second to (*R*)-BINOL.

Bibliography

1 M. Ratajczak-Sitarz, A. Katrusiak, K. Gawrońska and J. Gawroński, *Tetrahedron: Asymmetry*, 2007, **18**, 765–773.